Inorganica Chimica Acta 374 (2011) 578–585

Contents lists available at ScienceDirect

Inorganica Chimica Acta

journal homepage: www.elsevier.com/locate/ica

Origin of electronic absorption spectra of MLCT-excited and one-electron reduced 2,2′-bipyridine and 1,10-phenanthroline complexes

Stanislav Záliš [a,*], Cristina Consani [b], Amal El Nahhas [b], Andrea Cannizzo [b,1], Majed Chergui [b,*], František Hartl [c,*], Antonín Vlček Jr. [a,d,*]

[a] J. Heyrovský Institute of Physical Chemistry, Academy of Sciences of the Czech Republic, Dolejškova 3, CZ-182 23 Prague, Czech Republic
[b] Laboratoire de Spectroscopie Ultrarapide, ISIC, FSB-BSP, Ecole Polytechnique Fédérale de Lausanne, CH-1015 Lausanne-Dorigny, Switzerland
[c] Department of Chemistry, University of Reading, Whiteknights, Reading RG6 6AD, United Kingdom
[d] Queen Mary University of London, School of Biological and Chemical Sciences, Mile End Road, London E1 4NS, United Kingdom

ARTICLE INFO

Article history:
Available online 3 March 2011

Dedicated to Professor Wolfgang Kaim at the occasion of his 60th birthday.

Keywords:
TDDFT
Diimine
Spectroelectrochemistry
Rhenium complexes
Excited states

ABSTRACT

UV–Vis absorption spectra of one-electron reduction products and ^{3}MLCT excited states of [Re^{I}Cl(CO)$_3$(N,N)] (N,N = 2,2′-bipyridine, bpy; 1,10-phenanthroline, phen) have been measured by low-temperature spectroelectrochemistry and UV–Vis transient absorption spectroscopy, respectively, and assigned by open-shell TD-DFT calculations. The characters of the electronic transitions are visualized and analyzed using electron density redistribution maps. It follows that reduced and excited states can be approximately formulated as [Re^{I}Cl(CO)$_3$(N,N$^{\cdot-}$)]$^-$ and *[Re^{II}Cl(CO)$_3$(N,N$^{\cdot-}$)], respectively. UV–Vis spectra of the reduced complexes are dominated by IL transitions, plus weaker MLCT contributions. Excited-state spectra show an intense band in the UV region of ~50% IL origin mixed with LMCT (bpy, 373 nm) or MLCT (phen, 307 nm) excitations. Because of the significant IL contribution, this spectral feature is akin to the principal IL band of the anions. In contrast, the excited-state visible spectral pattern arises from predominantly LMCT transitions, any resemblance with the reduced-state visible spectra being coincidental. The Re complexes studied herein are representatives of a broad class of metal α-diimines, for which similar spectroscopic behavior can be expected.

1. Introduction

Electronic absorption spectra of MLCT excited states of α-diimine metal complexes are often similar to spectra of the reduced states, which, in turn resemble those of free α-diimine radical anions, N,N$^{\cdot-}$ [1]. Indeed, comparison of UV–Vis absorption as well as resonance Raman and IR spectra of reduced and excited states is used to assign and characterize the lowest excited state as MLCT [2–17]. This kind of experiments helped to establish that both reduction and MLCT excitation of [Ru^{II}(bpy)$_3$]$^{2+}$ are localized at a single bpy ligand, producing [Ru^{II}(bpy)$_2$(bpy$^{\cdot-}$)]$^+$ and *[Ru^{III}(bpy)$_2$(bpy$^{\cdot-}$)]$^{2+}$, respectively, instead of delocalized electronic structures [2,5,6,8,9,11,13,18]. In the case of mixed-ligand complexes, excited-state spectroscopy in combination with spectroelectrochemistry can reveal the localization of the excited electron. For example, observation of dpp$^{\cdot-}$ (dpp = 2,3-bis(2-pyridyl)pyrazine) UV–Vis features in the excited-state spectrum of a dinuclear complex [(bpy)$_2$Ru(μ-dpp)Ru(bpy)$_2$]$^{2+}$ provided an evidence that MLCT excitation is directed to the bridging ligand instead of bpy [19]. The similarities between UV–Vis spectroscopic effects of reduction and MLCT excitation are less obvious in complexes of 1,10-phenanthroline (phen) such as [Ru(phen)$_3$]$^{2+}$ [20] and [W(CO)$_4$(phen)] [15].

The very notion of the analogy between excited- and reduced-state spectra is based on the assumption that the same N,N$^{\cdot-}$ chromophore is present in both states. The same kind of ligand-localized π* orbital is occupied upon reduction and MLCT excitation (Scheme 1), leading to similar changes in intra-ligand bond lengths/strengths and causing the same qualitative changes in vibrational spectra. On the other hand, explaining analogous excited- and reduced-state UV–Vis spectral patterns would require making more assumptions: (i) interactions of metal d$_\pi$ with N,N$^{\cdot-}$ π and π* orbitals are very weak and comparable in the reduced and excited-states, (ii) the π and π* orbital energies are approximately the same or shift in the same direction on going from the reduced to the excited state, (iii) correlation and electron–electron interaction energies are comparable in both states, (iv) interconfigurational mixing between N,N$^{\cdot-}$-localized π → π* and other kinds of one-electron excitations is negligible. Some of

* Corresponding authors at: Queen Mary University of London, School of Biological and Chemical Sciences, Mile End Road, London E1 4NS, United Kingdom (A. Vlček).
E-mail addresses: zalis@jh-inst.cas.cz (S. Záliš), Majed.Chergui@epfl.ch (M. Chergui), f.hartl@reading.ac.uk (F. Hartl), a.vlcek@qmul.ac.uk (A. Vlček).
[1] Present address: Institute of Applied Physics, University of Bern, Sidlerstr. 5, CH-3012 Bern, Switzerland.

0020-1693/$ - see front matter © 2011 Elsevier B.V. All rights reserved.
doi:10.1016/j.ica.2011.02.084

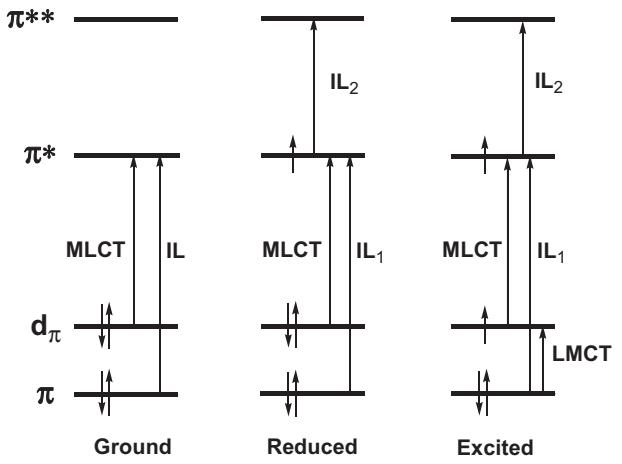

Scheme 1. Low-energy one-electron excitations of ground-, reduced-, and MLCT-excited states of closed-shell transition metal complexes. (Analogous schemes can be considered for complexes with L′LCT (ligand to ligand) or SBLCT (sigma-bond to ligand) lowest excited states [21–23] by replacing the d_π orbital by a ligand (L′) p_π and axial M–L′ σ orbital, respectively.)

these assumptions are hard to justify, considering that the total electron number is different in the excited- and reduced-state, the ligand-localized electron density experiences larger positive central field of the metal atom in the excited than in the reduced state, and the low-lying triplet excited states of polypyridine complexes generally are of a highly mixed character [24]. In addition, oxidation of the metal center in the MLCT excited state opens the possibility of LMCT transitions that cannot occur in the reduced state.

Curiously, the apparent analogy between excited- and reduced-state spectra were always used only as an empirical argument, without any serious attempt to examine its validity and physical origin. The nature of electronic transitions of reduced metal α-diimine complexes has not been studied by quantum chemical calculations and their generally accepted assignment to intraligand $N,N^{\cdot-}$ $\pi\pi^*$ transitions was based on similarities with the spectra of free reduced ligands. Excited-state triplet–triplet electronic transitions were theoretically investigated only very recently for $[Ru(bpy)_3]^{2+}$ [25] and a series of rhenium tricarbonyl bpy and phen complexes [26,27], using open-shell time-dependent DFT techniques (TD-DFT). Important contributions from LMCT excitations and character mixing appear to be common features of their excited-state transitions.

An important question emerges, as to whether the presumed spectroscopic analogy of reduced and excited states has a real physical basis or is only coincidental. Solving this problem will advance our understanding of electronic structures of reduced and excited α-diimine complexes. It will show to which extent the $N,N^{\cdot-}$ ligand can be treated as a quasi-isolated chromophoric unit, and whether observation of similar excited- and reduced-state spectra can really be used as diagnostic of the MLCT character of the excited state. We address these questions by comparing experimental UV–Vis absorption spectra and TD-DFT-calculated electronic transitions of excited states of two Re^{I} carbonyl diimines $[ReCl(CO)_3(N,N)]$ with those of the corresponding anions $[ReCl(CO)_3(N,N)]^-$ (N,N = phen, bpy). These compounds serve as excellent models to investigate reduction and excitation effects since they contain only a single electron-accepting diimine ligand, avoiding thus the localization problem ubiquitous in Ru^{II}-diimine chemistry [28,29]. Their electrochemical behavior is well known [4,30–34], and the lowest excited state character was firmly established by numerous experimental [4,21,26,27,35–46] as well as theoretical studies [24,42,43,47–49] as $ReCl(CO)_3 \rightarrow N,N$ ^{3}CT with a minor $\pi \rightarrow \pi^*(N,N)$ intraligand (IL) component. Below, it will be demonstrated that the reduced- and excited-state spectra indeed show features of analogous origin in the UV region but the visible absorption bands are of a different nature, mostly IL and LMCT, respectively.

2. Experimental

2.1. Materials

$[ReCl(CO)_3(bpy)]$ and $[ReCl(CO)_3(phen)]$ were prepared by standard procedures [35,36,39] and characterized by comparing their IR and ^{1}H NMR spectra with the literature data. Spectroscopic-grade solvents were used for all measurements. THF was freshly distilled from a sodium/benzophenone mixture before use. The supporting electrolyte, tetrabutylammonium hexafluorophosphate (TBAH, Aldrich) was recrystallized twice from absolute ethanol and dried overnight under vacuum at 80 °C.

2.2. Spectroelectrochemistry

Reduction was performed in a temperature-controlled spectroelectrochemical OTTLE cell of a 0.2 mm optical path [50,51] in THF at 253 K. The electrolysis potential was carefully controlled with a PA4 potentiostat (Laboratorní přístroje, Polná, Czech Republic) to avoid high Faradaic currents. UV–Vis and IR spectra were recorded on a Scinco S3100 diode array spectrophotometer and a Bruker Vertex 70v FT-IR spectrometer, respectively. The smooth isosbestic conversion of $[ReCl(CO)_3(N,N)]$ to the corresponding radical anion reached typically ~90%. At higher conversions, both UV–Vis and IR spectra showed emerging absorption of the 2e-reduced species $[Re(CO)_3(N,N)]^-$. The reason for this behavior is the partial overlap of the two $1e^-$ cathodic waves in the thin-layer cyclic voltammograms, the onset of the second step being merely 100 mV beyond the maximum of the first cathodic wave of $[ReCl(CO)_3(N,N)]$ (for $v = 2$ mV s^{-1}). Concentrations used: 3×10^{-1} M TBAH, 1.75×10^{-3} M $[ReCl(CO)_3(bpy)]$ and 1.5×10^{-3} M $[ReCl(CO)_3(phen)]$.

2.3. Time-resolved UV–Vis absorption spectra (TA)

Excited-state spectra were obtained as described previously [26,27,52]. In short, spectra in the visible spectral range were measured using 400 nm pumping (~100 fs, 1 kHz) and white-light continuum probe beam (340–680 nm) that was generated by focusing a small part of the 800 nm fundamental output of the Ti:S laser into a 1 mm thick CaF_2 window. TA spectra in the deep UV region were obtained using broadband UV pulses generated by achromatic frequency doubling of a NOPA output [53]. Sample absorbance was adjusted to 0.2–0.3 at 400 nm in a 0.2 mm flow cell. In both spectral regions, the relative polarization of the pump and probe light was set at the magic angle (54.7°). Intensities of the probe light transmitted by a pumped and unpumped sample were recorded alternately by a 512-pixel Si single diode array using a mechanical chopper in the pump beam path.

2.4. Quantum chemical calculations

Electronic structures were calculated by density functional theory (DFT) method using the GAUSSIAN 09 [54] program package. The geometries of the doublet ground state of $[ReCl(CO)_3(N,N)]^-$ and the lowest triplet excited state of $[ReCl(CO)_3(N,N)]$ (N,N = bpy, phen) were calculated by the UKS approach. DFT calculations employed Perdew, Burke, Ernzerhof [55,56] hybrid functional. For H, C, N, and O atoms, either polarized triple-ζ basis sets 6-311g(d)

[57] (geometry optimization) or cc-pvdz correlation consistent polarized valence double-ζ basis sets [58] (calculations of spectral transitions) were used. The Re orbitals were described with quasi-relativistic effective core pseudopotentials and the corresponding optimized set of basis functions [59,60]. Geometry optimizations were followed by vibrational analyses in order to characterize stationary states. The solvent was described by the polarizable continuum model (PCM) [61]: THF and DMF for the reduced and excited state, respectively. Low-lying excitation energies were calculated by time-dependent DFT (TD-DFT) at the optimized geometry. The difference density plots were drawn using the GaussView software.

3. Results and discussion

3.1. Spectroscopy of the reduced and excited states

$[Re^{I}Cl(CO)_3(N,N)]$ (N,N = bpy, phen) are reduced by one electron at −1.38 V versus SCE to the corresponding anions $[ReCl(CO)_3(N,N)]^-$ that undergo slow Cl^- ligand substitution by a donor solvent or dimerization [4,30–34]. The reduction becomes fully reversible at low temperatures [31] where the anions are stable and can be characterized spectroscopically. A second reduction and loss of the axial ligand occur at more negative potentials, producing $[Re(CO)_3(N,N)]^-$.

IR (Fig. 1) and UV–Vis (Figs. 2 and 3) spectra of both $[ReCl(CO)_3(N,N)]^-$ were obtained by reduction of $[Re^{I}Cl(CO)_3(N,N)]$ in an OTTLE cell at a carefully controlled potential to avoid contamination by the second reduction product. Performing the reduction at low temperature (253 K) stabilized the product against Cl^- ligand dissociation. Reoxidation at the corresponding anodic counterpeak fully regenerated the original spectra, proving that the complexes stay intact during the spectroelectrochemical experiments. In accordance with previous studies [4,30,32–34], we describe the reduction as predominantly ligand-localized, producing complexes of radical-anionic polypyridine ligands N,N$^{\cdot-}$: $[Re^{I}Cl(CO)_3(N,N^{\cdot-})]^-$. This assignment is fully supported by IR spectroelectrochemistry (Fig. 1) that shows only moderate shifts of ν(CO) bands to lower energies upon reduction (Table 1), indicating that the Re atom in the anionic complexes keeps its formal oxidation state I while it is exposed to a stronger electron donation from the reduced N,N$^{\cdot-}$ ligand.

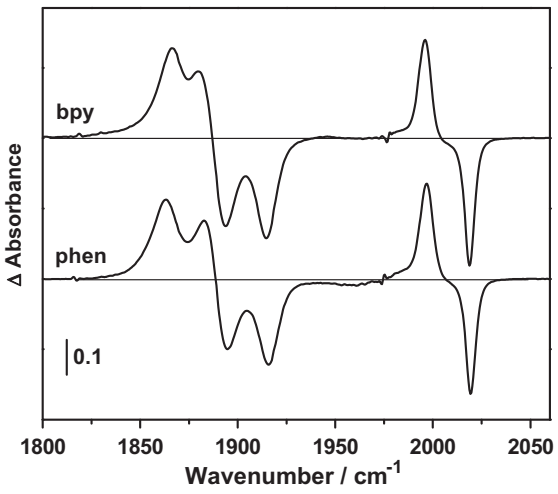

Fig. 1. Difference IR absorption spectra in the ν(CO) region obtained after ~90% spectroelectrochemical reduction of $[ReCl(CO)_3(bpy)]$ (top) and $[ReCl(CO)_3(phen)]$ (bottom) to the corresponding anions in THF/3 × 10^{-1} M TBAH at 253 K. Negative and positive peaks correspond to the parent and reduced complexes, respectively.

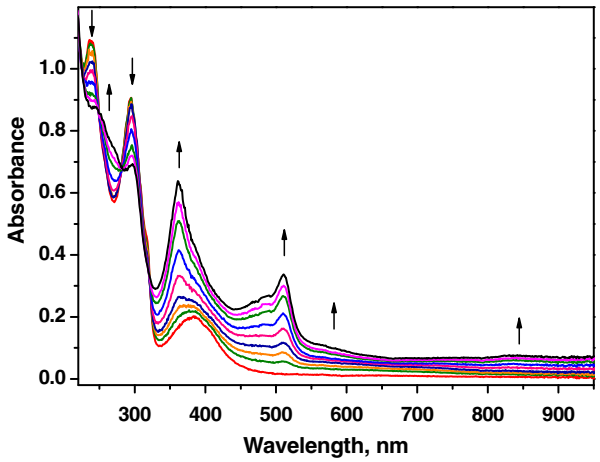

Fig. 2. UV–Vis absorption spectra recorded in the course of the one-electron reduction of $[ReCl(CO)_3(bpy)]$ in THF/3 × 10^{-1} M TBAH at 253 K. The first line (red) was recorded without applied potential. (For interpretation of the references to colour in this figure legend, the reader is referred to the web version of this article.)

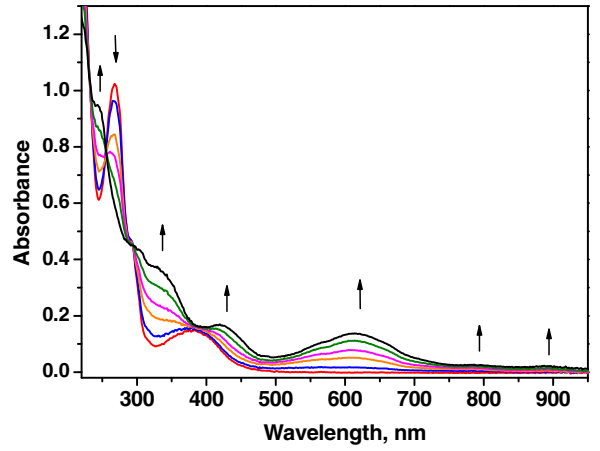

Fig. 3. UV–Vis absorption spectra recorded in the course of the one-electron reduction of $[ReCl(CO)_3(phen)]$ in THF/3 × 10^{-1} M TBAH at 253 K. The first line (red) was recorded without applied potential. (For interpretation of the references to colour in this figure legend, the reader is referred to the web version of this article.)

UV–Vis spectra (Figs. 2–5) of the parent complexes show a band due to $ReCl(CO)_3 \rightarrow$ N,N ^{1}CT transitions [48] at ~380 nm for both bpy and phen, followed by a predominantly IL $\pi\pi^*$ band that occurs at a longer wavelength for bpy than for phen: 295 and 267 nm, respectively. During reduction, these bands are gradually replaced by new ones at 361, 400(sh) 486(sh), 511, and 561 (sh) nm for $[Re^{I}Cl(CO)_3(bpy^{\cdot-})]^-$ and at 241(sh), ~307(sh), 420, and 614 nm for $[Re^{I}Cl(CO)_3(phen^{\cdot-})]^-$. In addition, both reduced species show fairly weak and broad absorption in the red and NIR regions.

The UV–Vis spectral pattern of $[Re^{I}Cl(CO)_3(bpy^{\cdot-})]^-$ resembles that of free bpy$^{\cdot-}$, characterized by bands at 391, 432(sh), 547, and 585 nm [62], as well as spectra of other reduced metal complexes such as $[Cr(CO)_4(bpy^{\cdot-})]^-$ [14] or $[Ru(bpy)_3]^+$, the latter being formulated [5,6,11,18,34] as $[Ru^{II}(bpy)_2(bpy^{\cdot-})]^+$. The UV–Vis spectral features of $[Re^{I}Cl(CO)_3(phen^{\cdot-})]^-$ are comparable to those of free phen$^{\cdot-}$ [15]: an intense band at 360 nm, a shoulder at 415 nm, and a broad band at 575 nm. The $[Re^{I}Cl(CO)_3(phen^{\cdot-})]^-$ spectrum is rather different from that of $[W(CO)_4(phen^{\cdot-})]^-$, which exhibits a broad absorption feature in the 560–760 nm range with a resolved vibronic structure and a maximum at 604 nm, together with a strong absorption below 500 nm steadily increasing into the UV [15].

Table 1
Experimental and calculated CO stretching frequencies of $[ReCl(CO)_3(N,N)]$ and $[ReCl(CO)_3(N,N)]^-$.

Complex	Symmetry	Calculated[a] (cm^{-1})			Experimental (cm^{-1})		
		$n = 0$	$n = -1$	Δ	$n = 0$	$n = -1$	Δ
$[ReCl(CO)_3(bpy)]^n$	A′	1893	1860	−33	1893	1867	−26
	A″	1912	1874	−39	1915	1882	−33
	A′	2017	1991	−26	2019	1996	−23
$[ReCl(CO)_3(phen)]^n$	A′	1893	1860	−33	1894	1864	−30
	A″	1912	1874	−38	1916	1885	−31
	A′	2017	1992	−25	2020	1997	−23

[a] Scaling factor 0.957.

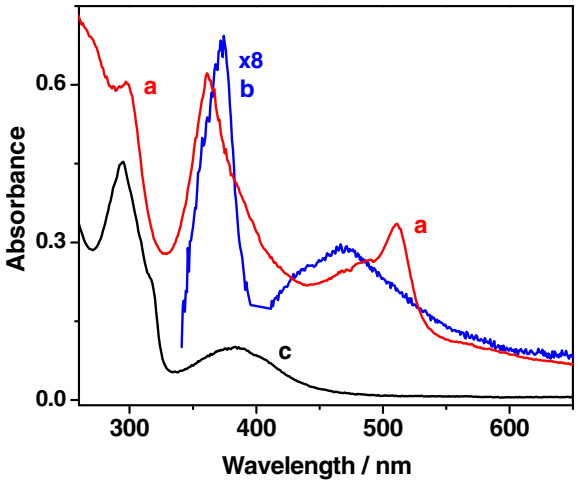

Fig. 4. UV–Vis absorption spectra of the reduced (a, red), excited (b, blue), and ground (c, black) states of $[ReCl(CO)_3(bpy)]$. The excited-state spectrum (recorded at a time delay of 45 ps with respect to the 400 nm, 100 fs pump pulse) is displayed as a difference absorption spectrum. Signal between 395 and 411 nm was removed to avoid contamination by scattered excitation light. The excited-state spectrum was measured in DMF at 293 K. The ground- and reduced-state spectra were obtained in THF/3 × 10^{-1} M TBAH at 253 K. The reduced-state spectrum is corrected for the residual 10% ground-state absorption. (For interpretation of the references to colour in this figure legend, the reader is referred to the web version of this article.)

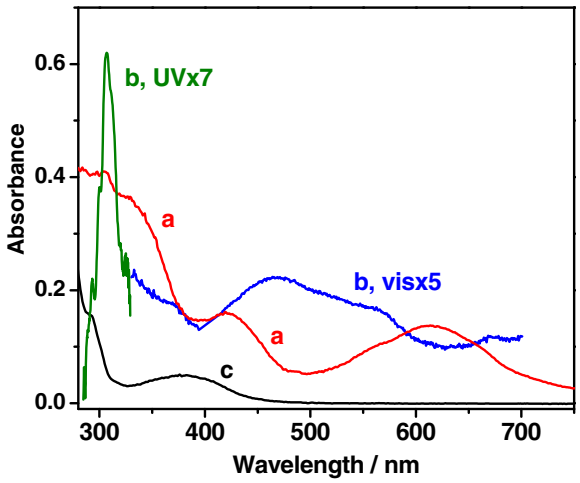

Fig. 5. UV–Vis absorption spectra of the reduced (a, red), excited (b, blue, olive), and ground (c, black) states of $[ReCl(CO)_3(phen)]$. The excited-state spectrum is displayed as a difference absorption spectrum. UV (olive) and visible (blue) spectra were obtained in separate experiments at time delays of 160 and 65 ps, respectively, after the 400 nm, ~100 fs pump pulse. Signal between 394 and 416 nm was removed to avoid contamination by scattered excitation light. The excited-state spectrum was measured in DMF at 293 K. The ground- and reduced-state spectra were obtained in THF/3 × 10^{-1} M TBAH at 253 K. The reduced-state spectrum is corrected for the residual 10% ground-state absorption. (For interpretation of the references to colour in this figure legend, the reader is referred to the web version of this article.)

The UV–Vis spectra of the reduced complexes are compared in Figs. 4 and 5 with the experimental excited-state difference absorption spectra. The latter represent the difference of the absorption of the excited sample minus that of the ground state. They are displayed in this form because extraction of pure excited-state absorption spectra requires a prior knowledge of the photoexcitation yield, which is not available. Nevertheless, the comparisons with the reduced-state spectra can be made because: (a) the ground state absorption set in at 450 nm, so that any new features at longer wavelengths are not affected by the ground state absorption; (b) the features that show up at wavelengths shorter than 450 nm are all new excited-state absorption bands, since they overwhelm the ground state absorption in this region (shown in black). Excited-state spectra (blue, olive) were measured at a sufficiently long time delay (>40 ps) after excitation, which (given the ultrafast rate of relaxation processes in these systems [26,27,40]) ensures that they represent the relaxed lowest excited state.

The excited-state spectrum of $[ReCl(CO)_3(bpy)]$ displays the typical [4,26,27,40] strong narrow band at 373 nm, and a weaker broad band at ~466 nm with a shoulder at ~440 nm. Whereas the intense near-UV bands of the excited and reduced states are comparable in appearance, the shapes of the corresponding absorption features in the visible indicate different origins. The excited-state spectrum of $[ReCl(CO)_3(phen)]$ shows a strong band at 307 nm with shoulders at 300 and 312 nm. (The absorption band is skewed below 300 nm by overlapping strong ground-state bleach.) In the visible spectral region, a broad absorption occurs between 450 and 600 nm with a maximum at 470 nm and a distinct shoulder at ~565 nm. The excited-state UV–Vis spectral pattern is clearly different from that of the reduced $[Re^{I}Cl(CO)_3(phen^{\cdot-})]^-$. The strong absorption at ~310 nm is the only common feature, although the excited-state band is sharper.

3.2. Origin of excited- and reduced-state electronic transitions: TD-DFT calculations

The structures of both reduced complexes in THF were calculated by DFT. Vibrational analysis has confirmed that they correspond to true energy minima. Calculated ν(CO) vibrational energies match well the experimental values determined spectroelectrochemically, Table 1. Excited-state calculations in DMF were described before [26,27,48]. Fig. 6 compares the calculated electronic transitions of both states. Characters of the transitions were deduced from the accompanying electron-density changes, shown in Figs. 7 and 8. It should be noted that they visualize very well all kinds of CT transitions [24] but may fail for those IL transitions that involve excitation between orbitals localized to a comparable extent at the same regions of the ligand. To overcome this problem, the transitions also were analyzed by inspecting both the

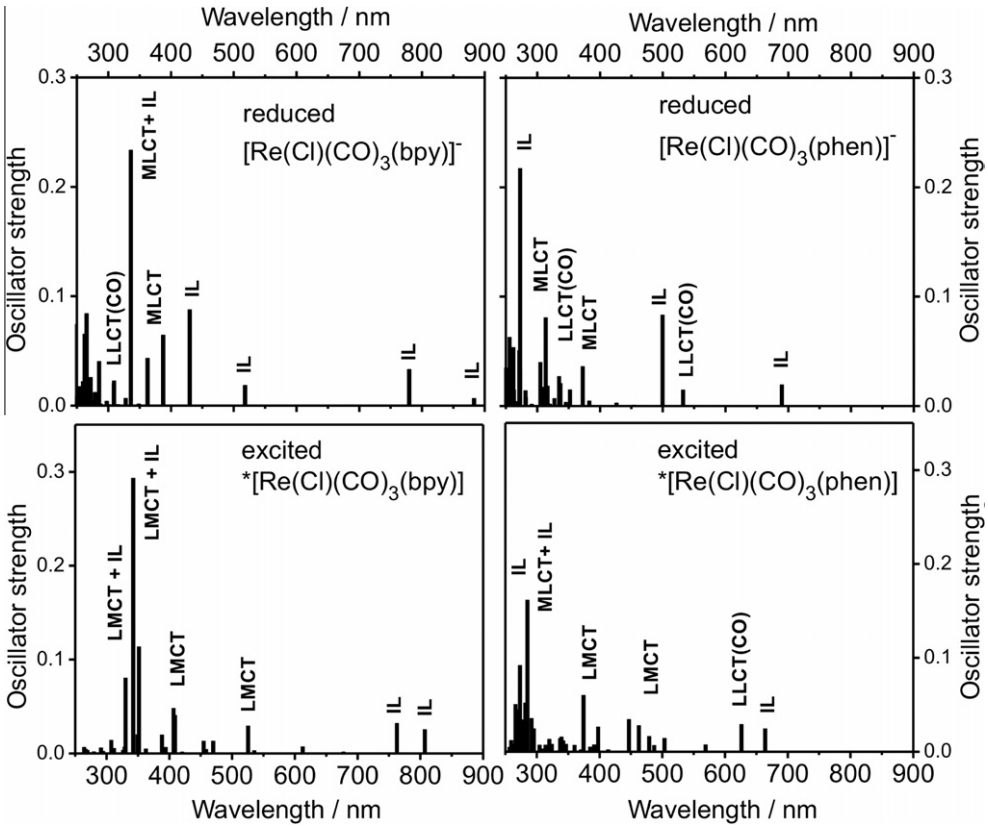

Fig. 6. Calculated electronic transitions for reduced (top) and excited (bottom) $[ReCl(CO)_3(N,N)]$ complexes.

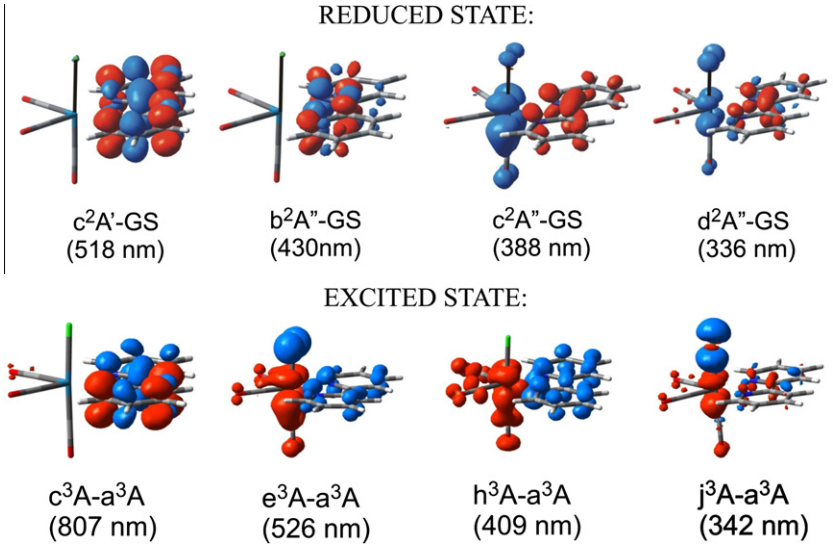

Fig. 7. Electron-density differences upon selected electronic transitions from the doublet ground state a^2A' of $[Re^{I}Cl(CO)_3(bpy^{\cdot-})]^-$ (top) and from the lowest excited state a^3A of $[ReCl(CO)_3(bpy)]$ (bottom). Regions of decreasing and increasing electron density are displayed in blue and red, respectively. Energies, principal excitations, and oscillator strengths of the excited-state triplet-triplet transitions are tabulated in [27] (symmetry-free calculation) and [26] (constrained C_s symmetry).

electron-density differences and the contributing one-electron excitations between individual molecular orbitals, see, for example, Fig. 9. The resulting predominant transition characters are then described by the labels in Fig. 6. A simplified "MLCT" notation is used for $ReCl(CO)_3 \rightarrow N,N/N,N^{\cdot-}$ excitations, which always contain significant "L′LCT" contribution due to electronic depopulation of the Cl ligand.

Spin density localized at the N,N ligand of $[ReCl(CO)_3(N,N)]$ was calculated to increase by 0.955 (0.954) and 1.035 (1.021) upon reduction and excitation, respectively, for N,N = bpy (phen). Population analysis thus confirms that the reduced and excited states can be formulated as containing the $N,N^{\cdot-}$ ligand: $[Re^{I}Cl(CO)_3(N,N^{\cdot-})]^-$ and $^*[Re^{II}Cl(CO)_3(N,N^{\cdot-})]$, respectively.

TD-DFT calculated electronic transitions of the anions (Table 2 and Fig. 6 – top panels) reproduce the main features seen in the experimental spectra, although the calculated transition energies are slightly shifted to higher energies relative to the experiment. The strong near-UV band of $[Re^{I}Cl(CO)_3(bpy^{\cdot-})]^-$ at 361 nm

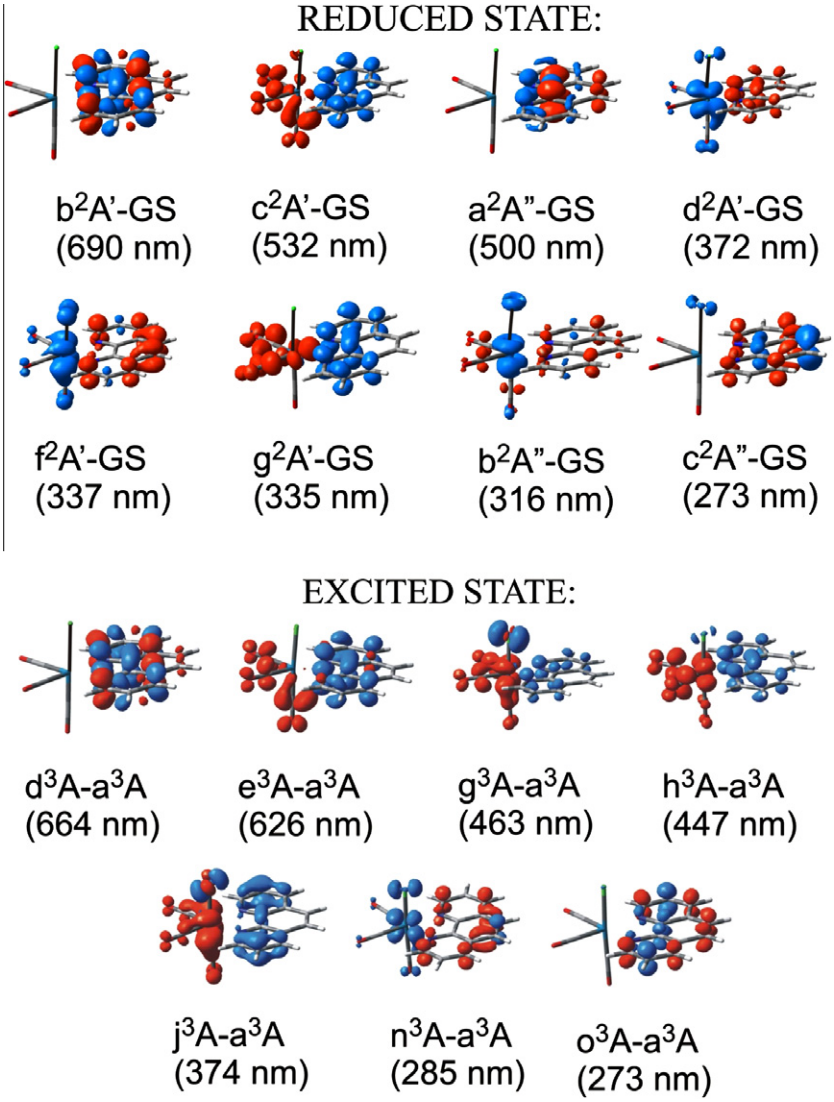

Fig. 8. Electron-density differences upon selected electronic transitions from the doublet ground state a^2A' of $[ReCl(CO)_3(phen^{\cdot-})]^-$ (top) and from the lowest excited state a^3A of $[ReCl(CO)_3(phen)]$ (bottom). Regions of decreasing and increasing electron density are displayed in blue and red, respectively. Energies, principal excitations, and oscillator strengths of the excited-state triplet–triplet transitions are tabulated in [27].

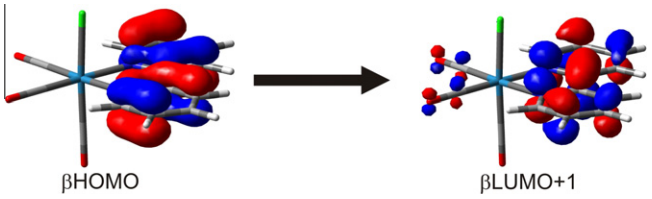

Fig. 9. Representation of the IL one-electron excitation contributing *ca.* 50 % to the intense $a^3A \rightarrow j^3A$ transition calculated at 342 nm for the lowest excited state of $[Re(Cl)(CO)_3(bpy)]$.

(calculated 336 nm) is due to the $a^2A' \rightarrow d^2A''$ transition of a mixed IL–MLCT/L'LCT character (Fig. 7) arising from a combination of $\pi \rightarrow \pi^*(bpy^{\cdot-})$ and $ReCl(CO)_3 \rightarrow bpy^{\cdot-}$ MLCT excitations, respectively. The latter accounts for the transition-energy dependence on the metal fragment: 391 nm (free $bpy^{\cdot-}$ [62]); 361 nm ($[Re^{I}Cl(CO)_3(bpy^{\cdot-})]^-$); 342 nm ($[Ru(bpy)_3]^+$ [6] and $[Cr(CO)_4(bpy)]^-$ [14]). The band broadening around 400 nm is due to MLCT transitions to d^2A' and c^2A'', whereas the distinct shoulder at 481 nm is attributed to the $a^2A' \rightarrow b^2A''$ IL transition (calculated at 430 nm), and the broad visible absorption feature around 500 nm is due to several vibronic transitions to the c^2A' IL state.

The intense broad UV band of $[Re^{I}Cl(CO)_3(phen^{\cdot-})]^-$ arises from a group of close-lying MLCT and IL transitions, the c^2A'' (calculated at 273 nm) being the most intense one. It is a predominantly IL transition with a small $Cl \rightarrow phen^{\cdot-}$ L'LCT contribution, Fig. 8. The broad bands around 420 and 614 nm are due to groups of $Re\text{-}Cl(CO)_3 \rightarrow phen^{\cdot-}$ MLCT and IL transitions, respectively. The spectra also contain less intense contributions from LLCT(CO) transitions c^2A' (532 nm) and g^2A' (335 nm) that arise from $phen^{\cdot-} \rightarrow Re(CO)_3$ excitations, delocalizing the excited electron density over the CO ligands, Figs. 7 and 8. Overall, it follows that the UV–Vis spectral patterns of the reduced complexes are generally determined by IL transitions of the $N,N^{\cdot-}$ ligand, whose energies and intensities are slightly altered relative to the free radical-anions. MLCT and, for the phen complex, LLCT(CO) transitions contribute to the spectra but do not change their overall pattern. In conclusion, TD-DFT analysis supports the analogy between electronic spectra of reduced diimine complexes and free radical anionic ligands $N,N^{\cdot-}$, while stressing that $N,N^{\cdot-}$ electronic transitions are affected by coordination.

Table 2
Calculated doublet–doublet excitation energies of $[ReCl(CO)_3(N,N)]^-$ both with oscillator strengths larger than 0.01. Transitions originate from the UKS-optimized doublet ground state a^2A'.

N,N	Final state	Assignment	Transition energy eV (nm)	Osc. str.	Expt. (nm)
bpy	b^2A'	IL ($bpy^{\cdot-}$)	1.41 (882)	0.010	
	a^2A''	IL ($bpy^{\cdot-}$)	1.59 (780)	0.033	
	c^2A'	IL ($bpy^{\cdot-}$)	2.39 (518)	0.019	
	b^2A''	IL ($bpy^{\cdot-}$)	2.88 (430)	0.088	
	c^2A''	MLCT	3.20 (388)	0.065	~400
	d^2A'	MLCT	3.42 (363)	0.044	~400
	d^2A''	MLCT + IL ($bpy^{\cdot-}$)	3.69 (336)	0.234	361
	e^2A'	LLCT(CO)	4.01 (309)	0.023	
	f^2A'	MLCT(CO)	4.01 (309)	0.021	
phen	b^2A'	IL ($phen^{\cdot-}$)	1.79 (690)	0.019	
	c^2A'	LLCT(CO)	2.33 (532)	0.015	614
	a^2A''	IL ($phen^{\cdot-}$)	2.48 (500)	0.084	614
	d^2A'	MLCT	3.33 (372)	0.036	420
	e^2A'	MLCT	3.52 (352)	0.015	420
	f^2A'	MLCT	3.68 (337)	0.021	
	g^2A'	LMCT + LLCT(CO)	3.50 (335)	0.027	
	h^2A'	LLCT(CO)	3.92 (316)	0.019	
	b^2A''	MLCT	3.96 (316)	0.081	
	c^2A''	IL ($phen^{\cdot-}$)	4.55 (273)	0.218	307
	i^2A'	MLCT + IL ($phen^{\cdot-}$)	4.55 (273)	0.034	241

Next, we will compare the characters of calculated electronic transitions of the reduced and the excited state of each complex, attempting to find and elucidate their common features as well as differences. Perusal of Figs. 4–6 reveals that the only region where the reduced- and excited-state spectra show a meaningful resemblance both in appearance and origin is in the UV, around 360–380 nm for $[ReCl(CO)_3(bpy)]$ and ~310 nm for $[ReCl(CO)_3(phen)]$. In the case of excited $[ReCl(CO)_3(bpy)]$, the strong near-UV band arises predominantly from the close-lying transitions i^3A and j^3A. Electron-density differences (Fig. 7) indicate a $Cl \rightarrow Re^{II}$ LMCT character, while analysis of contributing excitations reveals ~50% IL contribution, Fig. 9. The UV transitions of excited $[ReCl(CO)_3(phen)]$ are of a mixed IL–MLCT origin with smaller $Cl,phen^{\cdot-} \rightarrow Re^{II}(CO)_3$ LMCT admixtures. The IL character predominates in the $a^3A' \rightarrow o^3A$ transition, Fig. 8. The broader UV absorption of the reduced than excited $[ReCl(CO)_3(phen)]$ is due to a group of near-UV MLCT transitions of the anion that are absent in the excited state. Contrary to the reduced state, IL transitions do not determine the excited-state spectral pattern in the visible region. Instead, the visible absorption features arise mostly from LMCT transitions due to $N,N^{\cdot-} \rightarrow Re^{II}(CO)_3$ and $Cl \rightarrow Re^{II}(CO)_3$ excitations. Individual transitions differ in the relative contributions of these two excitations and the extent of delocalization of the excited electron density over the CO ligands, i.e. the LLCT(CO) contribution. Low-lying IL excitations localized at the $N,N^{\cdot-}$ ligand make admixtures to several of these LMCT and LLCT(CO) transitions but do not give rise to the typical IL spectral pattern seen in the reduced state.

4. Conclusions

Spectroelectrochemistry and TD-DFT analysis have confirmed the correspondence between UV–Vis spectra of free $bpy^{\cdot-}$ and $phen^{\cdot-}$ radical anions on one hand and reduced complexes $[Re^{I}Cl(CO)_3(bpy^{\cdot-})]^-$ and $[Re^{I}Cl(CO)_3(phen^{\cdot-})]^-$ on the other. Intraligand $\pi\pi^*$ transitions of the $N,N^{\cdot-}$ ligands determine the spectral patterns of the reduced complexes. Weaker MLCT and (for phen) LLCT(CO) transitions also contribute to the spectra, manifested mainly by broadening of the IL bands. In the case of $[Re^{I}Cl(CO)_3(bpy^{\cdot-})]^-$, the transition responsible for the characteristic sharp near-UV band is of a mixed IL–MLCT character, whereas the corresponding, predominantly IL, band of $[Re^{I}Cl(CO)_3(phen^{\cdot-})]^-$ occurs deeper in the UV, being partly obscured by a group of close-lying MLCT transitions.

On going from the reduced to the excited state, the strong UV band persists, but the underlying IL transition acquires significant CT admixtures. Lower-lying MLCT transitions vanish from the spectra as the metal atom gets oxidized. Surprisingly, the low-energy IL transitions in the visible spectral region vanish as well. Instead, a manifold of LMCT transitions emerges, arising from mixed excitations of electron density from $N,N^{\cdot-}$ and/or the axial Cl ligand to the oxidized $Re^{II}(CO)_3$ moiety, combined with smaller IL admixtures. The LMCT transitions determine the pattern of the excited-state spectra in the visible region. We can thus conclude that there is a correspondence between reduced- and excited-state spectra of α-diimine complexes in the UV, whereas any similarities seen in the visible spectral region are only coincidental. In fact, such similarities are apparent only for the bpy complexes; excited- and reduced-state spectra of $[Re^{I}Cl(CO)_3(phen)]$ are rather different, even at first sight.

The occurrence of $Re^{I}Cl(CO)_3 \rightarrow N,N^{\cdot-}$ MLCT transitions at relatively low energies in the anionic complexes shows that the $N,N^{\cdot-}$ ligands retain the π electron-accepting character of the parent α-diimines. At the same time, they act as π-donors, as is manifested by LMCT/L′LCT transitions transferring electron density to the $Re^{II}(CO)_3$ unit in the excited states. (The $phen^{\cdot-}$ ligand seems to be even more versatile since $[ReCl(CO)_3(phen)]$ shows MLCT and L′LCT(CO) transitions in both the excited and reduced state.)

Results obtained herein for Re carbonyl α-diimine complexes can easily be generalized to understand the UV–Vis spectroscopic behavior of reduced and excited complexes of other metals and α-diimines. Observation of a strong sharp band in the excited-state spectrum resembling that of a reduced $\alpha\text{-diimine}^{\cdot-}$ or of the corresponding reduced metal complex is a good indication of ligand reduction upon excitation, i.e. of an MLCT, LLCT, or an SBLCT excited state. On the other hand, no conclusions on the excited-state character can be based on comparing the visible spectra alone. Moreover, the extensive overlap between absorption spectra of excited and reduced states should be considered when studying photoinduced electron transfer in supramolecular systems containing α-diimine chromophores by UV–Vis time-resolved absorption spectroscopy. In many cases, it will be hard to distinguish the reduced from the excited state of the chromophore, and kinetics measured at a single wavelength will likely contain contributions from the excited-state decay, as well as forward and back electron

transfer. Clearly, spectra and kinetics of such systems should be studied over broad spectral ranges, combining spectroelectrochemical and time-resolved spectroscopic experiments.

Acknowledgments

Funding was provided by the Ministry of Education of the Czech Republic Grants LD11086 and LD11082, QMUL, the University of Reading, the Swiss NSF via the NCCR MUST, and by the European collaboration program COST D35 and the European Science Foundation DYNA network.

References

[1] A. Vlček Jr., Chemtracts – Inorg. Chem. 5 (1993) 1.
[2] P.S. Braterman, A. Harriman, G.A. Heath, L.J. Yellowlees, J. Chem. Soc., Dalton Trans. (1983) 1801.
[3] M. Forster, R.E. Hester, Chem. Phys. Lett. 81 (1981) 42.
[4] K. Kalyanasundaram, J. Chem. Soc., Faraday Trans. 2 (82) (1986) 2401.
[5] C.M. Elliott, E.J. Hershenhart, J. Am. Chem. Soc. 104 (1982) 7519.
[6] G.A. Heath, L.J. Yellowlees, P.S. Braterman, J.C.S. Chem. Commun. (1981) 287.
[7] C.M. Elliott, J.C.S. Chem. Commun. (1980) 261.
[8] W.H. Woodruff, R.F. Dallinger, J. Am. Chem. Soc. 101 (1979) 4391.
[9] P.G. Bradley, N. Kress, B.A. Hornberger, R.F. Dallinger, W.H. Woodruff, J. Am. Chem. Soc. 103 (1981) 7441.
[10] W.K. Smothers, M.S. Wrighton, J. Am. Chem. Soc. 105 (1983) 1067.
[11] S.M. Angel, M.K. DeArmond, R.J. Donohoe, K.W. Hanck, D.W. Wertz, J. Am. Chem. Soc. 106 (1984) 3688.
[12] C.D. Tait, D.B. MacQueen, R.J. Donohoe, M.K. De Armond, K.W. Hanck, D.W. Wertz, J. Phys. Chem. 90 (1986) 1766.
[13] K.M. Omberg, J.R. Schoonover, J.A. Treadway, R.M. Leasure, R.B. Dyer, T.J. Meyer, J. Am. Chem. Soc. 119 (1997) 7013.
[14] J. Víchová, F. Hartl, A. Vlček Jr., J. Am. Chem. Soc. 114 (1992) 10903.
[15] E. Lindsay, A. Vlček Jr., C.H. Langford, Inorg. Chem. 32 (1993) 2269.
[16] N.H. Damrauer, J.K. McCusker, J. Phys. Chem. A 103 (1999) 8440.
[17] P. Chen, K.M. Omberg, D.A. Kavaliunas, J.A. Treadway, R.A. Palmer, T.J. Meyer, Inorg. Chem. 36 (1997) 954.
[18] M.K. DeArmond, K.W. Hanck, D.W. Wertz, Coord. Chem. Rev. 64 (1985) 65.
[19] R.M. Berger, Inorg. Chem. 29 (1990) 1920.
[20] C. Turró, Y.C. Chung, N. Leventis, M.E. Kuchenmeister, P.J. Wagner, G.E. Leroi, Inorg. Chem. 35 (1996) 5104.
[21] D.J. Stufkens, A. Vlček Jr., Coord. Chem. Rev. 177 (1998) 127.
[22] M. Turki, C. Daniel, S. Záliš, A. Vlček Jr., J. van Slageren, D.J. Stufkens, J. Am. Chem. Soc. 123 (2001) 11431.
[23] C. Daniel, Coord. Chem. Rev. 230 (2002) 65.
[24] A. Vlček Jr., S. Záliš, Coord. Chem. Rev. 251 (2007) 258.
[25] M.-F. Charlot, Y. Pellegrin, A. Quaranta, W. Leibl, A. Aukauloo, Chem. Eur. J. 12 (2006) 796.
[26] A. El Nahhas, A. Cannizzo, F. van Mourik, A.M. Blanco-Rodríguez, S. Záliš, A. Vlček Jr., M. Chergui, J. Phys. Chem. A 114 (2010) 6361.
[27] A. El Nahhas, C. Consani, A.M. Blanco-Rodríguez, K.M. Lancaster, O. Braem, A. Cannizzo, M. Towrie, I.P. Clark, S. Záliš, M. Chergui, A. Vlček Jr., Inorg. Chem. 50 (2011) 2932.
[28] S. Wallin, J. Davidsson, J. Modin, L. Hammarström, J. Phys. Chem. A 109 (2005) 4697.
[29] J.K. McCusker, Acc. Chem. Res. 36 (2003) 876.
[30] J.C. Luong, L. Nadjo, M.S. Wrighton, J. Am. Chem. Soc. 100 (1978) 5790.
[31] F. Paolucci, M. Marcaccio, C. Paradisi, S. Roffia, C.A. Bignozzi, C. Amatore, J. Phys. Chem. B 102 (1998) 4759.
[32] F.P.A. Johnson, M.W. George, F. Hartl, J.J. Turner, Organometallics 15 (1996) 3374.
[33] G.J. Stor, F. Hartl, J.W.M. van Outersterp, D.J. Stufkens, Organometallics 14 (1995) 1115.
[34] A. Vlček Jr., in: V. Balzani, D. Astruc (Eds.), Electron Transfer in Chemistry, Wiley-VCH, Weinheim, 2001, p. 804.
[35] M.S. Wrighton, D.L. Morse, J. Am. Chem. Soc. 96 (1974) 998.
[36] L.A. Worl, R. Duesing, P. Chen, L. Della Ciana, T.J. Meyer, J. Chem. Soc., Dalton Trans. (1991) 849.
[37] M.W. George, F.P.A. Johnson, J.R. Westwell, P.M. Hodges, J.J. Turner, J. Chem. Soc., Dalton Trans. (1993) 2977.
[38] D.R. Gamelin, M.W. George, P. Glyn, F.-W. Grevels, F.P.A. Johnson, W. Klotzbücher, S.L. Morrison, G. Russell, K. Schaffner, J.J. Turner, Inorg. Chem. 33 (1994) 3246.
[39] B.D. Rossenaar, D.J. Stufkens, A. Vlček Jr., Inorg. Chem. 35 (1996) 2902.
[40] D.J. Liard, M. Busby, P. Matousek, M. Towrie, A. Vlček Jr., J. Phys. Chem. A 108 (2004) 2363.
[41] M. Busby, A. Gabrielsson, P. Matousek, M. Towrie, A.J. Di Bilio, H.B. Gray, A. Vlček Jr., Inorg. Chem. 43 (2004) 4994.
[42] A.M. Blanco-Rodríguez, A. Gabrielsson, M. Motevalli, P. Matousek, M. Towrie, J. Šebera, S. Záliš, A. Vlček Jr., J. Phys. Chem. A 109 (2005) 5016.
[43] A. Gabrielsson, M. Busby, P. Matousek, M. Towrie, E. Hevia, L. Cuesta, J. Perez, S. Záliš, A. Vlček Jr., Inorg. Chem. 45 (2006) 9789.
[44] D.M. Dattelbaum, K.M. Omberg, J.R. Schoonover, R.L. Martin, T.J. Meyer, Inorg. Chem. 41 (2002) 6071.
[45] D.M. Dattelbaum, K.M. Omberg, P.J. Hay, N.L. Gebhart, R.L. Martin, J.R. Schoonover, T.J. Meyer, J. Phys. Chem. A 108 (2004) 3527.
[46] K.A. Walters, Y.-J. Kim, J.T. Hupp, Inorg. Chem. 41 (2002) 2909.
[47] A. Vlček Jr., S. Záliš, J. Phys. Chem. A 109 (2005) 2991.
[48] A. Cannizzo, A.M. Blanco-Rodríguez, A. Nahhas, J. Šebera, S. Záliš, A. Vlček Jr., M. Chergui, J. Am. Chem. Soc. 130 (2008) 8967.
[49] R. Baková, M. Chergui, C. Daniel, A. Vlček Jr., S. Záliš, Coord. Chem. Rev. 255 (2011) 975.
[50] F. Hartl, H. Luyten, H.A. Nieuwenhuis, G.C. Schoemaker, Appl. Spectrosc. 48 (1994) 1522.
[51] T. Mahabiersing, H. Luyten, R.C. Nieuwendam, F. Hartl, Coll. Czech. Chem. Commun. 68 (2003) 1687.
[52] J. Helbing, L. Bonacina, R. Pietri, J. Bredenbeck, P. Hamm, F. van Mourik, F. Chaussard, A. Gonzalez-Gonzalez, M. Chergui, C. Ramos-Alvarez, C. Ruiz, J. Lopez-Garriga, Biophys. J. 87 (2004).
[53] C. Consani, M. Mirabelle Prémont-Schwarz, A. El Nahhas, C. Bressler, F. van Mourik, A. Cannizzo, M. Chergui, Angew. Chem., Int. Ed. 48 (2009) 7184–7187.
[54] M.J. Frisch, G.W. Trucks, H.B. Schlegel, G.E. Scuseria, M.A. Robb, J.R. Cheeseman, G. Scalmani, V. Barone, B. Mennucci, G.A. Petersson, H. Nakatsuji, M. Caricato, X. Li, H.P. Hratchian, A.F. Izmaylov, J. Bloino, G. Zheng, J.L. Sonnenberg, M. Hada, M. Ehara, K. Toyota, R. Fukuda, J. Hasegawa, M. Ishida, T. Nakajima, Y. Honda, O. Kitao, H. Nakai, T. Vreven, J.A. Montgomery Jr., J.E. Peralta, F. Ogliaro, M. Bearpark, J.J. Heyd, E. Brothers, K.N. Kudin, V.N. Staroverov, R. Kobayashi, J. Normand, K. Raghavachari, A. Rendell, J.C. Burant, S.S. Iyengar, J. Tomasi, M. Cossi, N. Rega, J.M. Millam, M. Klene, J.E. Knox, J.B. Cross, V. Bakken, C. Adamo, J. Jaramillo, R. Gomperts, R.E. Stratmann, O. Yazyev, A.J. Austin, R. Cammi, C. Pomelli, J.W. Ochterski, R.L. Martin, K. Morokuma, V.G. Zakrzewski, G.A. Voth, P. Salvador, J.J. Dannenberg, S. Dapprich, A.D. Daniels, O. Farkas, J.B. Foresman, J.V. Ortiz, J. Cioslowski, D.J. Fox, GAUSSIAN 09, Revision A.02, Gaussian, Inc., Wallingford, CT, 2009.
[55] J.P. Perdew, K. Burke, M. Ernzerhof, Phys. Rev. Lett. 77 (1996) 3865.
[56] C. Adamo, V. Barone, J. Chem. Phys. 110 (1999) 6158.
[57] K. Raghavachari, J.S. Binkley, R. Seeger, J.A. Pople, J. Chem. Phys. 72 (1980) 650.
[58] D.E. Woon, T.H. Dunning Jr., J. Chem. Phys. 98 (1993) 1358.
[59] D. Andrae, U. Häussermann, M. Dolg, H. Stoll, H. Preuss, Theor. Chim. Acta 77 (1990) 123.
[60] J.M.L. Martin, A. Sundermann, J. Chem. Phys. 114 (2001) 3408.
[61] J. Tomasi, B. Mennucci, R. Cammi, Chem. Rev. 105 (2005) 2999.
[62] M. Krejčík, A.A. Vlček, J. Electroanal. Chem. 313 (1991) 243.